RESEARCH PAPER

Acta Neurobiol Exp 2022, 82: 12–21
DOI: 10.55782/ane-2022-002

since 1928 ACTA NEUROBIOLOGIÆ EXPERIMENTALIS

LncRNA NEAT1 alleviates ischemic stroke *via* transcriptional inhibition of NLRP3 mediated by the miR-10b-5p/BCL6 axis

Zhi-Wen Zhou[1], Xiang Ren[1], Wen-Sheng Zhou[1], Ai-Ping Li[1], Li-Jun Zheng[2]*

[1] Departments of Neurology, Hunan Provincial People's Hospital, The First Affiliated Hospital of Hunan Normal University, Changsha, Hunan Province, China,
[2] Departments of Rehabilitation, Hunan Provincial People's Hospital, The First Affiliated Hospital of Hunan Normal University, Changsha, Hunan Province, China,
** Email: zhenglijun171211@sina.com*

Cerebral ischemic stroke (CIS) is a significant cause of disability and death. Inflammation usually occurs after CIS and accelerates cellular damage. NLRP3 plays a key role in the formation of CIS-associated inflammasome. Understanding how NLRP3 is regulated bears great importance. We hypothesized that lncRNA NEAT1 can downregulate NLRP3 expression by regulating the miR-10b-5p/BCL6 axis, and thus regulate microglia-driven inflammation. The expression of NEAT1 was analyzed in CIS patients and an *in vitro* model of oxygen and glucose deprivation/re-oxygenation (OGD/R). We assessed the levels of pro-inflammatory cytokines IL-18 and IL-1β with ELISA. Interactions between NEAT1/miR-10b-5p and miR-10b-5p/BCL6 were determined by luciferase assay. The interaction of BCL6 and NLRP3 was identified by ChIP; RNA, and protein levels were evaluated by qRT-PCR and western blot, respectively. We found that NEAT1 level was decreased in CIS patients and OGD/R treated cells. OGD/R exerted pro-inflammasome effects by increasing the expression of inflammasome-associated proteins and ROS and malondialdehyde (MDA) while inhibiting SOD production. This effect was partially antagonized by NEAT1. We bioinformatically identified interactions between NEAT1/miR-10b-5p, BCL6/miR-10b-5p, and NLRP3-promoter/BCL6, and validated them by luciferase assay, qRT-PCR, and ChIP. NEAT1 inhibited miR-10b-5p and upregulated BCL6 by ceRNA mechanism and alleviated OGD/R induced cell damage. We also proved that BCL6 was a repressive transcription factor in the regulation of NLRP3 expression. Thus, lncRNA NEAT1 inhibited inflammasome activation by NLRP3 in microglia via the NEAT1/miR-10b-5p/BCL6/NLRP3 regulatory axis, which alleviated deleterious outcomes of ischemic stroke.

Key words: LncRNA NEAT1, miR-10b-5p, inflammasome, cerebral ischemic stroke

INTRODUCTION

Cerebral ischemic stroke (CIS) accounts for more than 80% of all strokes and is the main cause of dementia, disability, and deaths (Musuka et al., 2015). CIS is usually caused by a sudden decrease in cerebral blood flow which leads to insufficient nutrient and oxygen supply, causing brain damage or cerebral infarction (Kunz and Iadecola, 2009). Carotid artery obstruction, large-artery atherosclerosis, cardiac arrest, chronic hypoxemia can all lead to CIS (Neumann et al., 2013). After CIS, immune cells including lymphocytes migrate to the affected area, promoting neural inflammation and accelerating damage of neurons. Anti-inflammatories are of great interest in exploring viable treatment options for stroke (Ismael et al., 2018). Understanding the regulatory mechanism of CIS-associated inflammation would provide valuable information for the development of treatment options of CIS.

Inflammasome refers to a complex that can activate caspase-1 and mediate the production of pro-inflammatory factors. For instance, IL-18 and IL-1β could both be

Received 6 January 2021, accepted 4 July 2021

activated by inflammasomes (Poznyak et al., 2020). It is considered that inflammasome plays an important role in CIS, and targeting inflammasome might be a treatment option for CIS patients (Liu et al., 2020). A recent study revealed that NOD-like receptor pyrin domain containing 3 (NLRP3) plays fundamental roles in mediating inflammasome formation and neuron injury during CIS associated inflammation and cellular death (Ismael et al., 2018). NLRP3 is a pattern recognition receptor (PRR) that can sense exogenous or endogenous pathogens and initiate responses of the innate immune system. After innate immune system activation, cytokines and chemokines are secreted to initiate inflammation and recruit immune cells to activate adaptive immune responses (Baragetti et al., 2020). However, the exact mechanism of how NLRP3 inflammasome is activated is not fully understood. For instance, tissue injury, infection, and many other exogenous factors could all lead to NLRP3 inflammasome activation (Zhou et al., 2010). Hence, exploring mechanisms of NLRP3 inflammasome regulation bears great importance and might reveal more targets and strategies for anti-CIS treatments. It was reported that BCL6 (B cell lymphoma 6) inhibited NLRP3 transcription and attenuate renal inflammation (Chen et al., 2017). Therefore, we asked whether BCL6 served a similar function in ischemic stroke.

LncRNA (long non-coding RNA) refers to non-coding RNAs with 200 nt in length. LncRNAs play important roles in regulating multiple biological processes such as epigenetic regulation, cell cycle regulation, apoptosis, and differentiation (Khorkova et al., 2015; St. Laurent et al., 2015; Chatterjee et al., 2017; Wang et al., 2018). It is commonly assumed that lncRNA exerted such functions through a ceRNA (competitive endogenous RNA) mechanism by immobilizing miRNA targets, decreases their concentration, and protects them from degradation, which eventually promotes expression of interrelated genes (Lin et al., 2020). During CIS, the regulatory role of lncRNA was also reported (Ghafouri-Fard et al., 2020). For example, the lncRNA SNHG12 could inhibit CIS-associated apoptosis through a miR-181a-5p/NEGR1 axis (Yan et al., 2020). The lncRNA SNHG16 modulated brain vascular damage associated with ischemia/reperfusion through the miR-15a-5p/BCL2 axis (Teng et al., 2020). The lncRNA HULC was associated with diseased risk and severity of CIS through a complex signal network (Chen et al., 2020). We previously reported that the lncRNA NEAT1 regulates CIS-associated inflammatory response and influences on survival and outcomes of CIS (Han and Zhou, 2019; Li et al., 2020). Besides, we have found that in oxygen-glucose deprivation (OGD) induced damage of cerebrum microvessels, NEAT1 promoted survival and angiogenesis through inhibiting miR-377 via a ceRNA mechanism which resulted in the upregulation of SIRT1, VEGFA and BCL-XL (Zhou et al., 2019). However, whether NEAT1 could exert a protective effect during CIS through other mechanisms need further exploration. We have previously identified a number of miRNAs as potential targets of NEAT1, including miR-10b-5p. miR-10b-5p is up-regulated in MCAO brain tissue or OGD treated neurons, and inhibiting the expression of miR-10b-5p can alleviate ischemic stroke (Wang et al., 2020b). BCL6 was also predicted as a target of miR-10b-5p. Hence, we speculated that NEAT1, miR-10b-5p, BCL6, and NLRP3 might form a regulatory axis in ischemic stroke.

In this paper, we demonstrate that NEAT1 can repress OGD/R-induced inflammation and oxidative stress in BV-2 (mice microglia cell line) by regulating miR-10b-5p/BCL6 axis-mediated inhibition of NLRP3 transcription. This study deepens our understanding of how CIS-associated NLRP3 inflammasome is regulated and might contribute to the development of new strategies for CIS treatment.

METHODS

Human serum sample collection

Serum from CIS patients and healthy volunteers were collected in Hunan Provincial People's Hospital. The informed consent has been obtained. This study was approved by the hospital's Ethical Committee and all experiments were designed and performed following the Declaration of Helsinki.

Cell culture and OGD/R treatment

BV-2 cells were purchased from ATCC and cultured in MEM medium + 10% fetal bovine serum (FBS) at 37°C with 5% CO_2. For OGD/R treatment, cells were cultured in glucose-free medium under a hypoxic condition (94% N_2, 5% CO_2, 1% O_2) for 4 h. Then these cells were re-oxygenated and cultured with MEM medium + 10% FBS under 21% O_2, 5% CO_2 for another 24 h.

Cell transfection and plasmids construction

The shRNA oligonucleotides against BCL6, mimics of miR-10b-5p, and controls nucleotides (NC) were synthesized and purchased from GenePharma (Shanghai, China). The cDNA of NEAT1 was acquired through RT-PCR. NEAT1 plasmid was constructed by linking

NEAT1 cDNA into pcDNA 3.1 (V79020, Invitrogen, USA). For transfection, required plasmids were mixed with lipofectamine 2000 (11668030, Invitrogen, USA) according to the manufacturer's instruction and transfected into indicated cells.

RNA extraction and real-time PCR

Total RNA extraction was completed by using TRIzol reagent (Invitrogen, USA). The cDNA of miR-10b-5p was acquired by reverse transcription using a microRNA reverse transcription kit (4366597, Applied Biosystem, USA). We also used the Taqman qPCR kit (4461884, Applied Biosystem, USA) to generate cDNA of the target mRNAs for qPCR. The qRT-PCR reaction was performed on ABI 7900 system using SYBR premix kit (RR820A, TaKaRa, Japan) following the manufacture's instructions. We analyzed the relative expression by normalizing target genes to GAPDH (as an internal control of mRNA) and U6 (as internal control as miRNA) using the $2^{-\Delta\Delta Ct}$ method, respectively.

NEAT1-F: 5'-GGGGCCACATTAATCACAAC-3',
NEAT1-R: 5'-CAGGGTGTCCTCCACCTTTA-3';
miR-10b-5p-F: 5'-CAGCAGCACACTGTGGTTTGTA-3',
miR-10b-5p-R: 5'-AACTGGTGTCGTGGAGTCGGC-3';
BCL6-F, 5'-TCCTCGGAAGATGAGATTGC-3',
BCL6-R, 5'-GTTGAGCACGATGAACTTGTA-3';
GAPDH-F: 5'-CGTGTTCCTACCCCCAATGT-3',
GAPDH-R: 5'-TGTCATCATACTTGGCAGGTTTCT-3';
U6-F: 5'-CTCGCTTCGGCAGCACA-3',
U6-R 5'-AACGCTTCACGAATTTGCGT-3'.

Western blot

Cells were lysed by RIPA (Sigma-Aldrich, USA). Protein samples were loaded on SDS-PAGE and separated for 200 V, 20 min, and 120 V 60 min. We then transfected proteins from PAGE gel onto nitrocellulose membranes. The membranes were firstly incubated with 5% BSA in TBST for blocking. Then, membranes were incubated with primary antibodies overnight at 4°C. The membranes were washed 3 times (5 min each time) by TBST on a shaker. Then, membranes were incubated with secondary antibodies on a shaker at room temperature in darkness for 60 min. Finally, protein bands were detected by enhanced chemiluminescence (ThermoFisher, USA) and the intensity of each band was analyzed in ImageJ. BCL6 (#14895), NLRP3 (#13158), ASC (#67824) and cleaved caspase-1 (#89332) antibodies were obtained from Cell Signaling Technology (CST, USA). All antibodies were diluted at 1:2000 in TBST with 5% BSA.

ROS assay

The detection of reactive oxygen species (ROS) was performed as previously described (Aranda et al., 2013). ROS production in BV-2 cells was measured using a microplate reader or fluorescence microscopy using 2',7'-dichlorofluorescein diacetate (H_2DCFDA) (D6883, Sigma-Aldrich) as fluorescent probes following the manufacturer's protocols.

Malondialdehyde (MDA) and superoxide dismutase (SOD) analysis

The level of MDA and SOD within BV-2 cells were detected using commercially available kits (MDA kit, BC0020; SOD kit, BC0170) purchased from Solarbio, Beijing, China following manufactures' instructions.

Dual-luciferase assay

The NLRP3 promoter plasmid sequences were generated and cloned into pmirGLO systems (E1330, Promega, USA), and the pGL3-basic vehicle vector was used as a control. Luciferase reporter system was transfected into 293T cells as indicated. Forty-eight hours post-transfection, cells were harvested and the relative luciferase activity was measured using Dual Luciferase Reporter Assay System (E1910, Promega, Wisconsin, USA). Experiments were conveyed following manufacturer's instruction.

ELISA assay

Concentrations of secreted IL-18 and IL-1β were detected using an ELISA kit (mlbio, ml063132, and ml063131). Firstly, we coated 96 well plates by incubating the plate overnight at 4°C with 100 µL diluted antibodies per well. The plate was then washed and loaded with blocking buffer and incubated for 1 h at room temperature. Solutions were removed from the plate and each well was loaded with samples or standards. Plates were incubated again at room temperature for 2 h, followed by 3 substrate solution washes. To stop the reaction, a stop solution was loaded into each well. Signals were detected under 450 nm.

Chromatin-immunoprecipitation (ChIP)

Briefly, ChIP was performed as follows. First, we prepared samples by incubating BV-2 cells with 1%

formaldehyde for 20 min. Cells were lysed using SDS buffer (1% SDS, 50 mM Tris-HCl pH 8.1, 10 mM EDTA) and the nuclei were isolated. Then, we incubated the BCL6 antibody with cellular lysate with sheared soluble chromatin at 4°C overnight and performed immunoprecipitation using protein A/G beads. Samples were de-crosslinked and the solutions containing DNA, RNase A and proteinase K were collected and subjected to qPCR. ChIP was performed using a commercial kit from Cell signaling technology (CST#9003). Briefly, cells were fixed with 4% paraformaldehyde for 10 min, collected, and lysed using SDS buffer (1% SDS, 50 mM Tris-HCl pH 8.1, 10 mM EDTA). The nucleus was isolated and incubated with a micrococcal nuclease to break down chromatin into fragments. Each sample was mixed with 100 µL of BCL6 antibody (#14895, Cell Signaling Technology) conjugated dynabeads and incubated overnight at 4°C on a rotating platform. Beads were collected with a magnetic particle concentrator and washed with RIPA buffer twice and with TE buffer once. Then we added 50 µL of elution buffer and vortexed samples briefly to resuspend the beads. Beads were incubated for 10 min at 65°C and vortexed briefly every 2 min during incubation. The tubes were centrifuged for 30 s at 11,000 g, and then we transferred the liquid to a new tube and added 120 µL of elution buffer to the supernatant in the new tube. Samples were de-crosslinked overnight in a 65°C incubator. DNA was purified and then resuspend in 30 µL of TE buffer containing 10 µg of RNase A and incubated for 2 h at 37°C. We purified the DNA using a QIAGEN QIA quick PCR purification kit (28104). The qRT-PCR was then performed to detect enrichment of promoter region of NLRP3. The following primers were used for NLRP3 ChIP PCR, forward: 5'-TCTCCATTGTGTCTTCTTGGTG-3'; reverse: 5'-CTGGGTGACAAGAGCAAGACT-3'.

Statistical analyses

In this study, experiments were repeated 3 times. Prism 6.0 software (GraphPad Software, USA) was used for data analyses. For comparison between the two groups, we used Student's t-test (two-tailed). To analyze differences among multiple groups, we used a one-way analysis of variance (ANOVA) followed by Tukey's *post hoc* test. We considered $P<0.05$ as statistically significant. Data are shown as the mean ± standard deviation (SD).

RESULTS

LncRNA NEAT1 is downregulated in CIS patients and OGD/R cell model

To investigate the expression of NEAT1 in OGD/R induced BV-2 cells and in serums from CIS patients, we conducted the following experiments. Firstly, we collected serums from a healthy population and CIS patients and detected NEAT1 expression by qRT-PCR. The expression of NEAT1 was significantly lower in CIS group compared with the healthy control group (Fig. 1A). Then, we conducted OGD/R (oxygen and glucose deprivation for 4 h and reoxygenate for 24 h) in mouse microglia cell line (BV-2), and detected NEAT1 expression by qPCR. Compared with the control group, OGD/R treated cells exerted lower NEAT1 expression

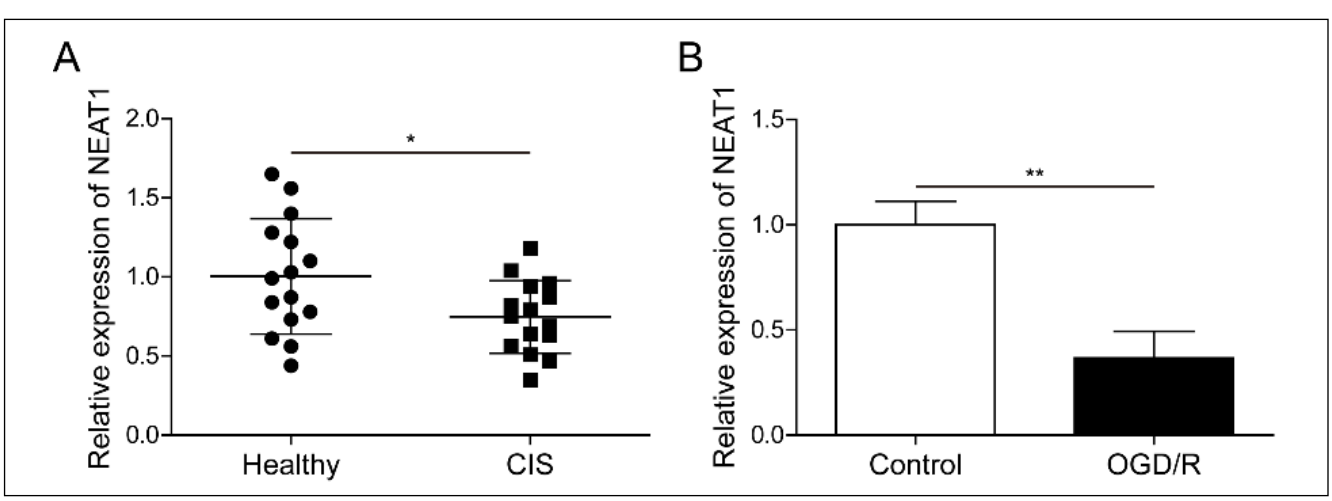

Fig. 1. lncRNA NEAT1 was downregulated in CIS patients and the H/R cell model. (A) NEAT1 levels in the serum samples of CIS patients and healthy controls were determined using qRT-PCR, n=15. *P<0.05. (B) BV-2 cells were subjected to OGD for 4 h followed by reoxygenation for 24 h. Thereafter, NEAT1 levels were measured using qRT-PCR. **P<0.01. Data are expressed as the mean ± SD. All experiments were replicated 3 times.

(Fig. 1B). These results indicated that NEAT1 was associated with CIS development.

NEAT1 overexpression alleviates OGD/R induced BV-2 cell injury

Then we transfected BV-2 cells with pcDNA-NEAT1 to evaluate the influences on OGD/R induced cellular damage. The transfection efficiency was confirmed using qRT-PCR. The results showed that NEAT1 overexpression indeed increased NEAT1 levels (Fig. 2A). Then, these cells were treated by OGD/R and subjected to western blot analysis to analyze the expression of inflammasome-associated proteins such as NLRP3, ASC, and cleaved caspase-1. These proteins were significantly elevated in OGD/R group, while the overexpression of NEAT1 inhibited OGD/R the upregulation of inflammasome-associated proteins (Fig. 2B). IL-1β and IL-18 in the supernatants were detected by ELISA assay to be

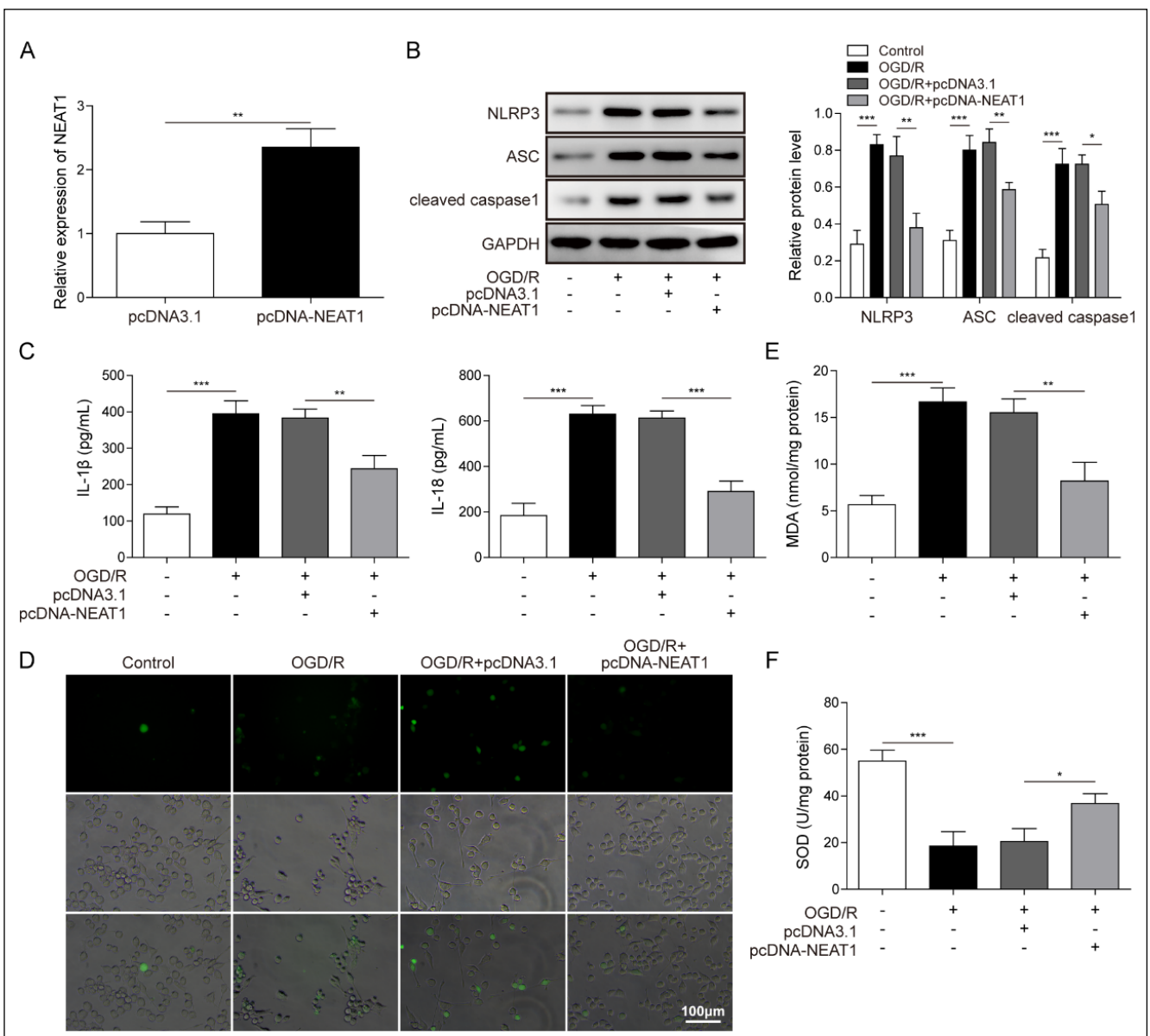

Fig. 2. NEAT1 overexpression alleviated OGD/R induced BV-2 cells injury. OGD/R treated BV-2 cells were transfected with pcDNA-NEAT1. (A) The transfection efficiency of NEAT1 was determined using qRT-PCR. (B) The levels of inflammasome-associated proteins NLRP3, ASC, and cleaved caspase-1 were detected by western blot. (C) The levels of IL-1β and IL-18 were determined by ELISA assay. (D-F) The ROS (D), MDA (E), and SOD (F) levels were determined by assay kits. Data are expressed as the mean ± SD. All experiments were replicated 3 times. *P<0.05; **P<0.01; ***P<0.001.

increased in the OGD/R group, which were alleviated by NEAT1 overexpression (Fig. 2C). Oxidative stress-associated markers such as ROS (reactive oxygen species), SOD (superoxide dismutase), and MDA (malondialdehyde) were also detected. Compared with the control group, OGD/R treated cells exerted increased ROS and MDA and decreased SOD, while NEAT1 overexpression alleviated such changes (Fig. 2D-F). From these results, we could speculate that NEAT1 overexpression alleviated OGD/R induced inflammatory damage and oxidative stress in BV-2 cells.

NEAT1 competitively interacted with miR-10b-5p and promoted the expression of BCL-6. To find the potential NEAT1 target, we adopted bioinformatic analysis using starBase, and the interaction sequence was identified between NEAT1 and miR-10b-5p (Fig. 3A). Because miR-10b-5p was predicted as NEAT1 target, we investigated whether it could interact with NEAT1. Dual luciferase reporter system containing wild type (NEAT1-wt) and mutant (NEAT1-mut) miR-10b-5p-interacting sequence of NEAT1 was constructed and co-transfected with miR-10b-5p into BV-2 cells. The luciferase activity was decreased in WT-NEAT1 group, which validated the interaction between NEAT1 and miR-10b-5p (Fig. 3B). Besides, the expression of miR-10b-5p was suppressed by NEAT1 overexpression (Fig. 3C). We also revealed the

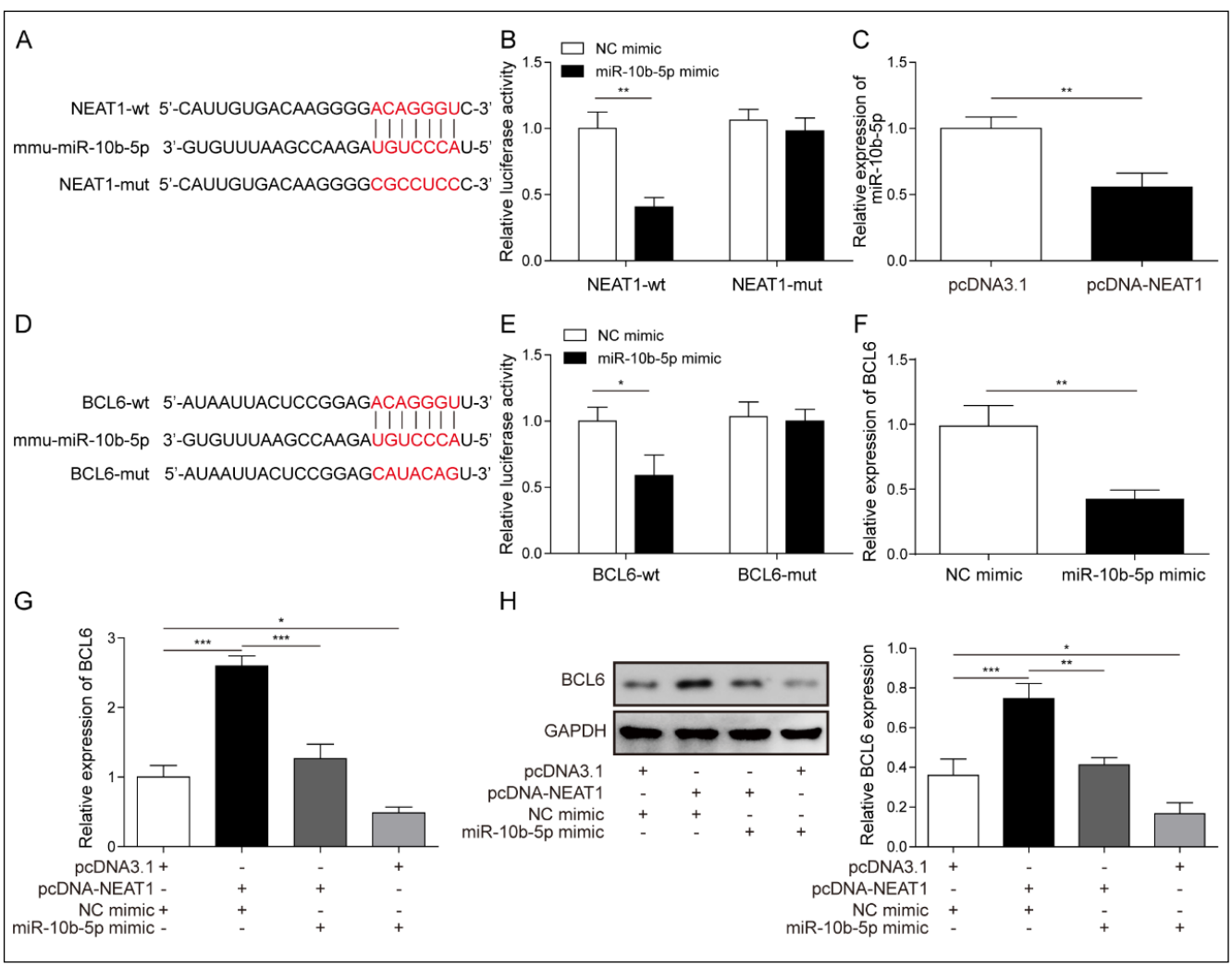

Fig. 3. NEAT1 competitively interacted with miR-10b-5p and promoted the expression of BCL-6. (A) starBase was used to predict the binding sequence between miR-10b-5p and NEAT1. (B) The interplay between miR-10b-5p and NEAT1 was validated using a dual-luciferase reporter assay. (C) The relative miR-10b-5p was estimated in pcDNA-NEAT1 or pcDNA3.1 transfected BV-2 cells by qRT-PCR. (D) starBase was used to predict the binding sequence between miR-10b-5p and BCL6. (E) The interplay between miR-10b-5p and BCL6 was verified using a dual-luciferase reporter assay. (F) The relative mRNA and (G) protein levels of BCL6 in pcDNA-NEAT1 or miR-10b-5p mimic transfected BV-2 cells were determined by qRT-PCR and western blot, respectively. Data are expressed as the mean ± SD. All experiments were replicated 3 times. *P<0.05; **P<0.01; ***P<0.001.

binding sequence between BCL6 and miR-10b-5p using starBase (Fig. 3D). Additionally, the luciferase activity of cells co-transfected with miR-10b-5p mimic and wild-type BCL6 (BCL6-wt) was notably decreased compared to that of cells co-transfected with a miR-10b-5p mimic and a mutant BCL6 vector (BCL6-mut) (Fig. 3E). Furthermore, BCL6 expression was promoted by NEAT1 overexpression and inhibited by transfection of miR-10b-5p mimic. NEAT1 overexpression partially rescued miR-10b-5p mimic induced BCL6 inhibition (Fig. 3F, G). Based on these evidence, we deduced that NEAT1 most likely acted as a ceRNA by targeting miR-10b-5p and promoting BCL6 expression.

NEAT1 alleviates OGD/R induced BV-2 cell injury by upregulating BCL-6 via inhibiting miR-10b-5p

In order to reveal whether NEAT1 affected OGD/R treated BV-2 cells through regulating the miR-10b-5p/BCL6 signaling axis, the following experiments were performed: BV-2 cells were transfected with NEAT1, miR-10b-5p mimic, and sh-BCL6 and subjected to western blot analysis to detect expression of inflammasome-associated proteins NLRP3, ASC, and cleaved caspase-1. OGD/R upregulated these proteins, while NEAT1 significantly inhibited the upregulation caused by OGD/R. In addition, miR-10b-5p overexpression partially abolished such function of NEAT1.

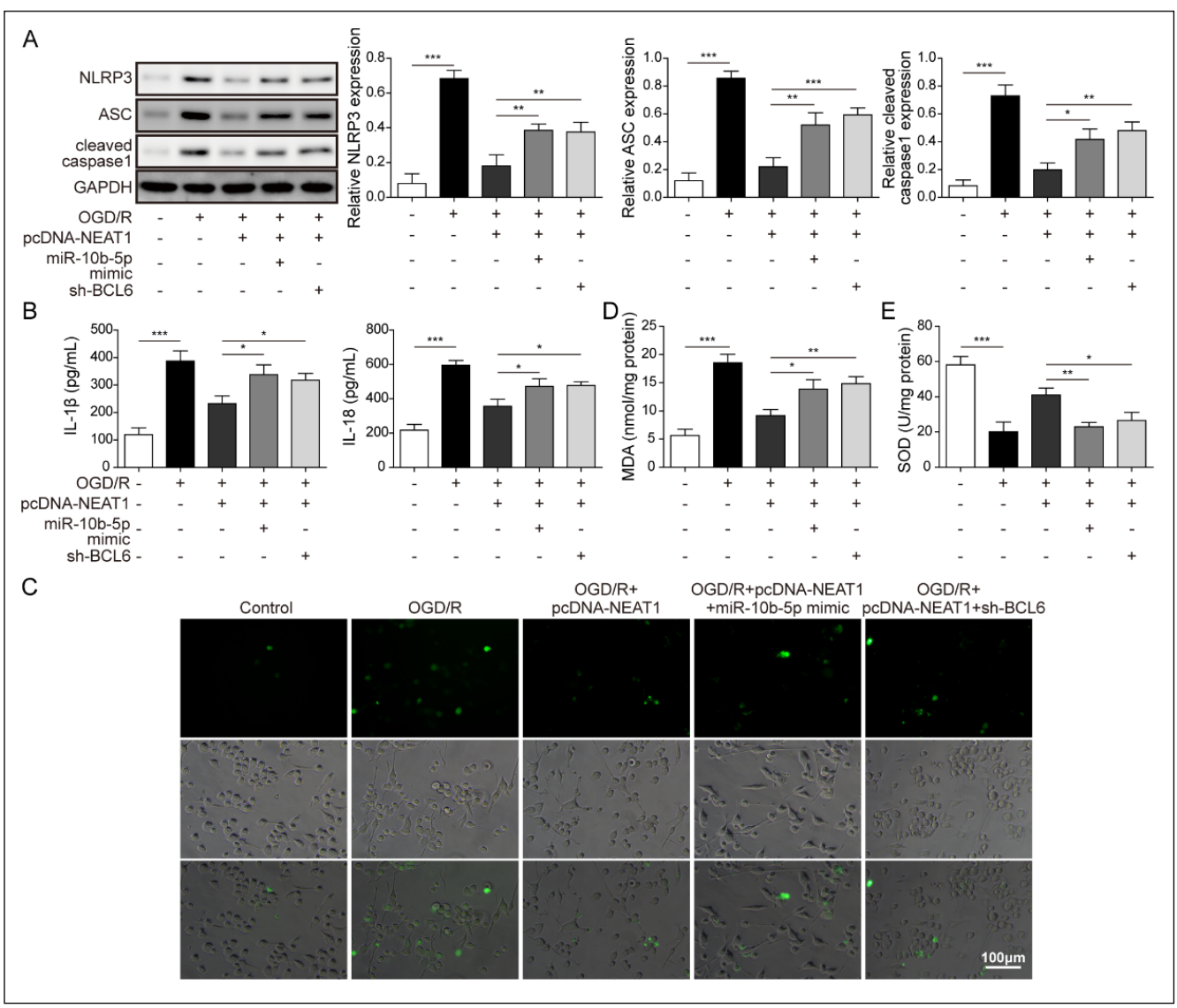

Fig. 4. NEAT1 alleviated OGD/R induced BV-2 cells injury by upregulating BCL6 expression via inhibiting miR-10b-5p. BV-2 cells under OGD/R condition were transfected with sh-BCL6, miR-10b-5p mimic or pcDNA-NEAT1. (A) The levels of inflammasome-associated proteins NLRP3, ASC, and cleaved caspase-1 were detected by western blot. (B) The levels of IL-1β and IL-18 were determined by ELISA assay. (C-E) The ROS (C), MDA (D), and SOD (E) levels were determined by assay kits. Data are expressed as the mean ± SD. All experiments were replicated 3 times. *P<0.05; **P<0.01; ***P<0.001.

Knockdown of BCL6 by sh-BCL6 exerted similar results with miR-10b-5p overexpression (Fig. 4A). NEAT1 overexpression significantly inhibited OGD/R induced secretion of IL-1β and IL-18 in the supernatants, while miR-10b-5p overexpression or sh-BCL6 attenuated the above effects of NEAT1 (Fig. 4B). Moreover, NEAT1 overexpression significantly inhibited OGD/R induced ROS, MDA, and suppressed SOD production, while miR-10b-5p overexpression or sh-BCL6 alleviated such function (Fig. 4C-E). Collectively, these data strongly suggested that NEAT1 alleviated OGD/R induced cellular injury by upregulating BCL-6 via inhibiting miR-10b-5p.

BCL6 inhibits transcription of NLRP3 and downregulates its expression

BCL6 is known as a transcription factor. In order to explore how did BCL6 regulate OGD/R induced BV-2 cells injury and to elucidate its downstream targets, we designed the following experiments. The binding site of BCL6 on the NLRP3 promoter was predicted by JASPAR software (Fig. 5A). The interaction between BCL6 and NLRP3 was analyzed by ChIP analysis. When BCL6 was knocked down by sh-BCL6, the signal corresponding to the NLRP3 transcription region was diminished, indicating a direct interaction between BCL6 and NLRP3 (Fig. 5B). Furthermore, dual-luciferase reporter assay was performed to investigate the interaction between NLRP3 promoter and BCL6. BCL6 knockdown promoted NLRP3 transcription which led to an increase in luciferase activity compared to the sh-NC group. While BCL6 knockdown had no effect on pGL3-basic (Fig. 5C). Next, we knocked down BCL6 using shRNA, and detected expression of BCL6 and NLRP3 using western blot and qPCR. BCL6 expression was significantly inhibited by sh-BCL6, while NLRP3 was significantly upregulated in both mRNA and protein levels (Fig. 5D, E). These results

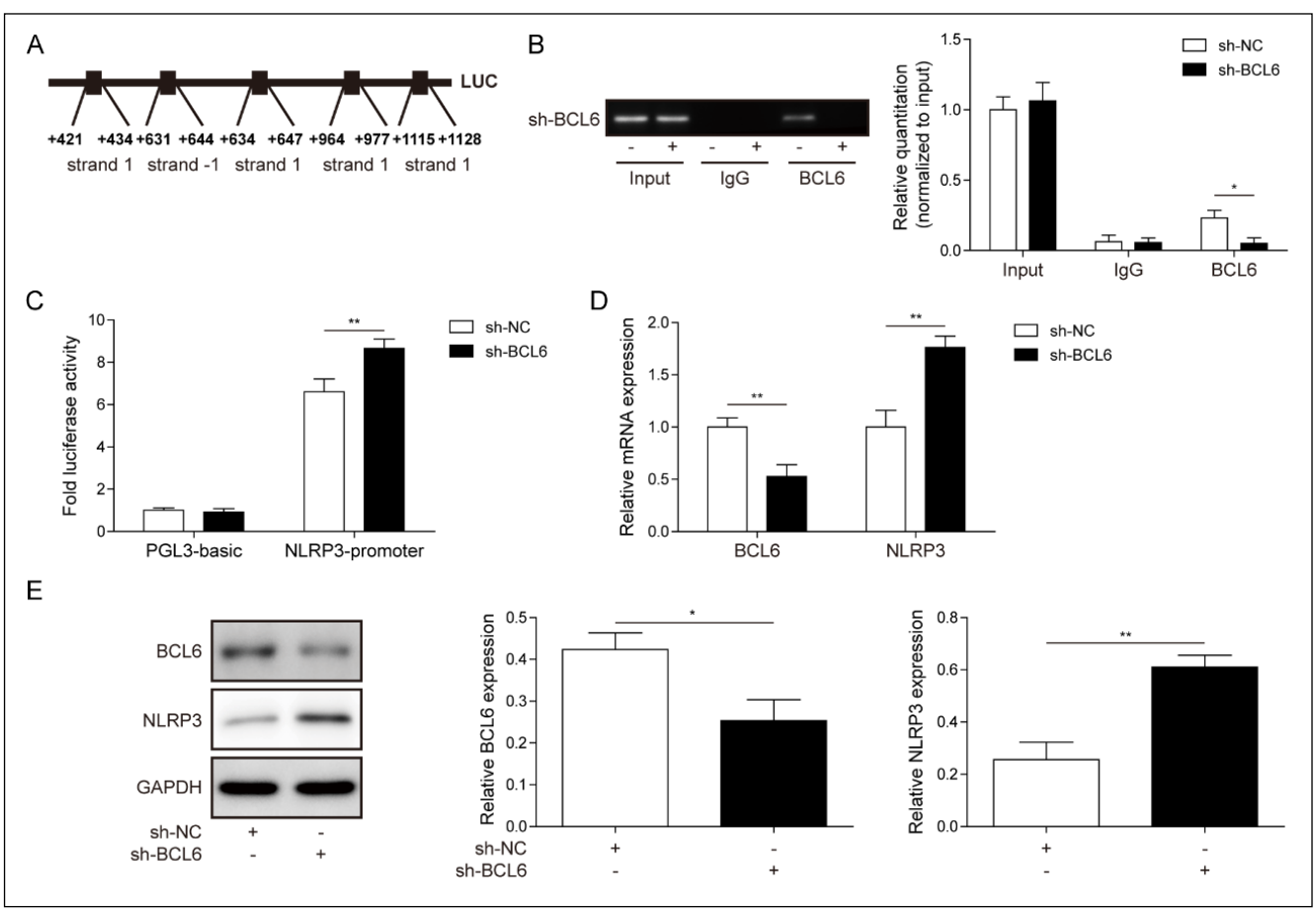

Fig. 5. BCL6 inhibited transcription of NLRP3 and suppressed its expression. (A) Potential interaction sites of BCL-6 in the promoter of NLRP3 were predicted by JASPAR software. (B) ChIP analysis showed the effects of BCL6-shRNA on the BCL6 binding to the NLRP3 promoter. (C) Dual-luciferase reporter assay was used to detect the NLRP3 gene promoter-reporter activity in cells transfected with sh-BCL6 or its corresponding control. (D-E) The mRNA and protein expression levels of BCL6 and NLRP3 after the knockdown of BCL6 were analyzed by qRT-PCR and Western blot. Data are expressed as the mean ± SD. All experiments were replicated 3 times. *P<0.05; **P<0.01.

demonstrated that BCL6 could inhibit NLRP3 transcription and translation.

DISCUSSION

Multiple lncRNAs have been reported in CIS with a plethora of proposed functions. For instance, Song and Kim (2020) discovered 5 differentially expressed lncRNA and more than 2000 differentially expressed miRNAs and these lncRNAs were potentially associated with CIS development through regulating apoptosis, inflammation, or other mechanisms. However, their expression pattern was different. For instance, lncRNA KCNQ1OT1 and lncRNA SHNG15 were increased after I/R (ischemia/reperfusion) injury in ischemic stroke patients or in a OGD-induced cell model (Guo et al., 2020; Wang et al., 2020a). In our study, we reported that lncRNA NEAT1 was down-regulated in serums of CIS patients and an *in vitro* OGD/R cell model. This indicated that different lncRNAs might function through different signaling pathways after CIS. When we overexpressed NEAT1, OGD/R induced cellular injuries were alleviated. These results were consistent with the previous report of NEAT1 in ischemic stroke, where elevated NEAT1 was associated with better prognosis and facilitated survival and angiogenesis in OGD induced brain microvascular endothelial cells (Zhou et al., 2019).

The widely accepted concept explaining how lncRNA regulated miRNA and downstream gene expression is the ceRNA (competing endogenous RNA) hypothesis (Lin et al., 2020). Briefly, lncRNAs harbor a vast amount of interaction sequences of certain miRNAs and could interact with them like a sponge, decreasing the free miRNA within the cytosol. Therefore, the miRNA was inhibited and its target gene was up-regulated. In this study, we revealed the binding sequences between miR-10b-5p and NEAT1, and proved their direct interaction by both qRT-PCR and dual-luciferase reporter assay. NEAT1 overexpression inhibited miR-10b-5p and upregulated its target gene BCL6. These results were consistent with the ceRNA mechanism. Although many miRNAs had been reported as NEAT1 targets, such as miR-326 in neuroblastoma (Yang et al., 2020), miR-23a in mononuclear cells (Rao et al., 2020), and miR-543 in chondrocyte (Xiao et al., 2020). miR-10b-5p was first discovered as a NEAT1 target, especially in CIS. It was noteworthy that Zhang and colleagues reported that NEAT1 could promote NLRP3 inflammasome in immune cells such as dendritic cells and macrophages, which was controversial with our results (Zhang et al., 2019a, Zhang et al., 2019b). However, in osteoblasts, NEAT1 could inhibit NLRP3 inflammasome and ameliorate inflammation, which was consistent with our finding (Dai et al., 2021). This was presumably due to a variety of functions and gene expression profiles among different cell types or diseases, and effects of NEAT1 varied among different diseases or cell lines accordingly.

BCL6 was previously reported with the function to attenuate inflammation (Chen et al., 2017). In our work, NEAT1 overexpression upregulated BCL6 expression and alleviated OGD/R induced cell inflammation damage and oxidative stress. BCL6 was previously reported as a transcription factor that can repress NOTCH2 and NOTCH pathway genes to maintain the survival of human follicular lymphoma cells (Valls et al., 2017). Recently, Ni et al found that BCL6 can negatively regulate cardiac fibroblast activation and function by directly binding to smad4 (Ni et al., 2019). Herein, we also revealed that BCL6 could directly interact with the promoter of NLRP3 and inhibit NLRP3 expression.

CONCLUSION

In summary, lncRNA NEAT1 inhibited inflammasome activation in microglia by inhibition of NLRP3 via a miR-10b-5p/BCL6 signaling pathway, which could influence outcomes of ischemic stroke. We report for the first time, that lncRNA NEAT1 acted as a sponge of miR-10b-5p, and BCL6 was a target of miR-10b-5p. We also uncovered the NEAT1/miR-10b-5p/BCL6/NLRP3 signaling pathway that was tightly associated with inflammation during CIS. These findings shed new light on our understanding of the regulatory mechanism of NEAT1 inflammasome during CIS, and might provide a potential therapeutic target for CIS treatment.

ACKNOWLEDGMENT

This work was supported by General Scientific Research Projects of Hunan Health Commission (No. 20200606) and Excellent Youth Project of Hunan Education Department (No. 20B375).

REFERENCES

Aranda A, Sequedo L, Tolosa L, Quintas G, Burello E, Castell JV, Gombau L (2013) Dichloro-dihydro-fluorescein diacetate (DCFH-DA) assay: a quantitative method for oxidative stress assessment of nanoparticle-treated cells. Toxicol In Vitro 27: 954–963.

Baragetti A, Catapano AL, Magni P (2020) Multifactorial activation of NLRP3 inflammasome: relevance for a precision approach to atherosclerotic cardiovascular risk and disease. Int J Mol Sci 21: 4459.

Chatterjee P, Roy D, Bhattacharyya M, Bandyopadhyay S (2017) Biological networks in Parkinson's disease: an insight into the epigenetic mechanisms associated with this disease. BMC Genomics 18: 721.

Chen D, Xiong XQ, Zang YH, Tong Y, Zhou B, Chen Q, Li YH, Gao XY, Kang YM, Zhu GQ (2017) BCL6 attenuates renal inflammation via negative regulation of NLRP3 transcription. Cell Death Dis 8: e3156.

Chen X, Zhang X, Su C, Huang S (2020) Long noncoding RNA HULC in acute ischemic stroke: Association with disease risk, severity, and recurrence-free survival and relation with IL-6, ICAM1, miR-9, and miR-195. J Clin Lab Anal 34: e23500.

Dai W, Wang M, Wang P, Wen J, Wang J, Cha S, Xiao X, He Y, Shu R, Bai D (2021) lncRNA NEAT1 ameliorates LPS-induced inflammation in MG63 cells by activating autophagy and suppressing the NLRP3 inflammasome. Int J Mol Med 47: 607–620.

Ghafouri-Fard S, Shoorei H, Taheri M (2020) Non-coding RNAs participate in the ischemia-reperfusion injury. Biomed Pharmacother 129: 110419.

Guo T, Liu Y, Ren X, Wang W, Liu H (2020) Promoting role of long non-coding RNA small nucleolar RNA host gene 15 (SNHG15) in neuronal injury following ischemic stroke via the microRNA-18a/CXC chemokine ligand 13 (CXCL13)/ERK/MEK axis. Med Sci Monit 26: e923610.

Han D, Zhou Y (2019) YY1-induced upregulation of lncRNA NEAT1 contributes to OGD/R injury-induced inflammatory response in cerebral microglial cells via Wnt/β-catenin signaling pathway. In Vitro Cell Dev Biol Anim 55: 501–511.

Ismael S, Zhao L, Nasoohi S, Ishrat T (2018) Inhibition of the NLRP3-inflammasome as a potential approach for neuroprotection after stroke. Sci Rep 8: 5971.

Khorkova O, Hsiao J, Wahlestedt C (2015) Basic biology and therapeutic implications of lncRNA. Adv Drug Deliv Rev 87: 15–24.

Kunz A, Iadecola C (2009) Cerebral vascular dysregulation in the ischemic brain. Handb Clin Neurol 92: 283–305.

Li P, Duan S, Fu A (2020) Long noncoding RNA NEAT1 correlates with higher disease risk, worse disease condition, decreased miR-124 and miR-125a and predicts poor recurrence-free survival of acute ischemic stroke. J Clin Lab Anal 34: e23056.

Lin W, Liu H, Tang Y, Wei Y, Wei W, Zhang L, Chen J (2020) The development and controversy of competitive endogenous RNA hypothesis in non-coding genes. Mol Cell Biochem 476: 109–123.

Liu H, Wu X, Luo J, Zhao L, Li X, Guo H, Bai H, Cui W, Guo W, Feng D, Qu Y (2020) Adiponectin peptide alleviates oxidative stress and NLRP3 inflammasome activation after cerebral ischemia-reperfusion injury by regulating AMPK/GSK-3β. Exp Neurol 329: 113302.

Musuka TD, Wilton SB, Traboulsi M, Hill MD (2015) Diagnosis and management of acute ischemic stroke: speed is critical. CMAJ 187: 887–893.

Neumann JT, Cohan CH, Dave KR, Wright CB, Perez-Pinzon MA (2013) Global cerebral ischemia: synaptic and cognitive dysfunction. Curr Drug Targets 14: 20–35.

Ni J, Wu QQ, Liao HH, Fan D, Tang QZ (2019) Bcl6 Suppresses cardiac fibroblast activation and function via directly binding to Smad4. Curr Med Sci 39: 534–540.

Poznyak AV, Melnichenko AA, Wetzker R, Gerasimova EV, Orekhov AN (2020) NLPR3 inflammasomes and their significance for atherosclerosis. Biomedicines 8: 205.

Rao Y, Fang Y, Tan W, Liu D, Pang Y, Wu X, Zhang C, Li G (2020) Delivery of long non-coding RNA NEAT1 by peripheral blood mononuclear cells-derived exosomes promotes the occurrence of rheumatoid arthritis via the microRNA-23a/MDM2/SIRT6 axis. Front Cell Dev Biol 8: 551681.

Song J, Kim YK (2020) Discovery and functional prediction of long non-coding RNAs common to ischemic stroke and myocardial infarction. J Lipid Atheroscler 9: 449–459.

St. Laurent G, Wahlestedt C, Kapranov P (2015) The Landscape of long noncoding RNA classification. Trends Genetics 31: 239–251.

Teng H, Li M, Qian L, Yang H, Pang M (2020) Long non-coding RNA SNHG16 inhibits the oxygen-glucose deprivation and reoxygenation-induced apoptosis in human brain microvascular endothelial cells by regulating miR-15a-5p/bcl-2. Mol Med Rep 22: 2685–2694.

Valls E, Lobry C, Geng H, Wang L, Cardenas M, Rivas M, Cerchietti L, Oh P, Yang SN, Oswald E, Graham CW, Jiang Y, Hatzi K, Agirre X, Perkey E, Li Z, Tam W, Bhatt K, Leonard JP, Zweidler-McKay PA, Maillard I, Elemento O, Ci W, Aifantis I, Melnick A (2017) BCL6 antagonizes NOTCH2 to maintain survival of human follicular lymphoma cells. Cancer Discov 7: 506–521.

Wang DQ, Fu P, Yao C, Zhu LS, Hou TY, Chen JG, Lu Y, Liu D, Zhu LQ (2018) Long non-coding RNAs, novel culprits, or bodyguards in neurodegenerative diseases. Mol Ther Nucleic Acids 10: 269–276.

Wang HJ, Tang XL, Huang G, Li YB, Pan RH, Zhan J, Wu YK, Liang JF, Bai XX, Cai J (2020a) Long non-coding KCNQ1OT1 promotes oxygen-glucose-deprivation/reoxygenation-induced neurons injury through regulating MIR-153–3p/FOXO3 Axis. J Stroke Cerebrovasc Dis 29: 105126.

Wang L, Liu W, Zhang Y, Hu Z, Guo H, Lv J, Du H (2020b) Dexmedetomidine had neuroprotective effects on hippocampal neuronal cells via targeting lncRNA SHNG16 mediated microRNA-10b-5p/BDNF axis. Mol Cell Biochem 469: 41–51.

Xiao P, Zhu X, Sun J, Zhang Y, Qiu W, Li J, Wu X (2020) LncRNA NEAT1 regulates chondrocyte proliferation and apoptosis via targeting miR-543/PLA2G4A axis. Hum Cell 34: 60–75.

Yan Y, Chen L, Zhou J, Xie L (2020) SNHG12 inhibits oxygen-glucose deprivation-induced neuronal apoptosis via the miR-181a-5p/NEGR1 axis. Mol Med Rep 22: 3886–3894.

Yang B, Ye X, Wang J, Xia S (2020) Long noncoding RNA nuclear-enriched abundant transcript 1 regulates proliferation and apoptosis of neuroblastoma cells treated by cisplatin by targeting miR-326 through Janus kinase/signal transducer and activator of transcription 3 pathway. Neuroreport 31: 871–878.

Zhang M, Zheng Y, Sun Y, Li S, Chen L, Jin X, Hou X, Liu X, Chen Q, Li J, Liu M, Zheng X, Zhang Y, Wu J, Yu B (2019a) Knockdown of NEAT1 induces tolerogenic phenotype in dendritic cells by inhibiting activation of NLRP3 inflammasome. Theranostics 9: 3425–3442.

Zhang P, Cao L, Zhou R, Yang X, Wu M (2019b) The lncRNA Neat1 promotes activation of inflammasomes in macrophages. Nat Commun 10: 1495.

Zhou R, Tardivel A, Thorens B, Choi I, Tschopp J (2010) Thioredoxin-interacting protein links oxidative stress to inflammasome activation. Nature Immunol 11: 136–140.

Zhou ZW, Zheng LJ, Ren X, Li AP, Zhou WS (2019) LncRNA NEAT1 facilitates survival and angiogenesis in oxygen-glucose deprivation (OGD)-induced brain microvascular endothelial cells (BMECs) via targeting miR-377 and upregulating SIRT1, VEGFA, and BCL-XL. Brain Res 1707: 90–98.